Characterization of Solution and Solid State Properties of Undoped and Doped Polyanilines Processed from Hexafluoro-2-propanol

Alan R. Hopkins and Paul G. Rasmussen*

Center for Macromolecular Science and Engineering and Department of Chemistry, The University of Michigan, Ann Arbor, Michigan 48109-1055

Rafil A. Basheer

Polymers Department, General Motors Research and Development Center, Warren, Michigan 48090-9055

ABSTRACT: We have investigated the changes in the molecular conformation, morphology, and conductivity of polyaniline as it transforms from the insulating emeraldine base (PANI-EB) to the conducting emeraldine salt (PANI-ES) in solutions of hexafluoro-2-propanol (HFIP) and in films processed from the same solvent. Since *both* PANI-EB and PANI-ES dissolve in this *single* solvent, we are able to observe for the first time conformational changes as a function of the molar doping level, *y*. HFIP both solvates and complexes PANI-EB (i.e., $y = 0$) which promotes a disruption in secondary interactions between chains and allows individual polyaniline chains to adopt a more expanded molecular conformation. As PANI-EB is fully doped to PANI-ES (i.e., $y = 0.50$), a decrease in the GPC retention time and an increase in [η] argues in favor of an expanded chain conformation in HFIP. When the solvent is removed (under very mild conditions) from PANI-ES, the expanded molecular conformation is retained in the solid state, based on the strong absorption of the UV−vis/near-IR free carrier tail at 2500 nm and good room temperature conductivity. The results in this study indicate that the HFIP solvent can be used to process PANI-EB and PANI-ES with diversified dopant counteranions; in some cases, enhanced optical, conductivity, and morphology properties result from the use of this solvent.

I. Introduction

The emeraldine base form of polyaniline (PANI-EB) is an alternating copolymer of reduced and oxidized dimer segments
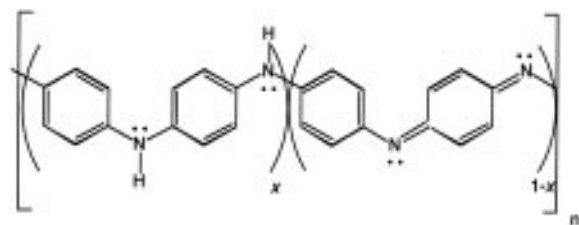
where $x \approx 0.5$. When the imine nitrogens are stoichiometrically doped or protonated to the molar doping ratio of 0.5 (e.g., using 1 mol of a nonoxidizing Brønsted acid, relative to 2 mol of Ph−NH repeat unit), the alternating copolymer transforms to a polyconjugated polyradical cation salt with an average of two radical cation charge carriers (i.e., polarons) per tetrameric repeating unit which are stabilized with dopant counteranions (A⁻). This conductive form of polyaniline, typically labeled polyaniline emeraldine salt (PANI-ES), is as follows:
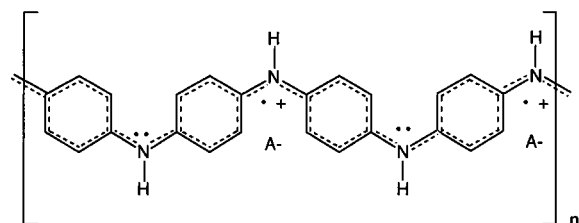
* To whom correspondence should be addressed.
⊗ Abstract published in *Advance ACS Abstracts,* October 15, 1996.

When PANI-EB is doped (i.e., protonated) to the PANI-ES form, the polymer undergoes an insulator-to-metal transition with a concomitant conformational change in the polymer backbone to accommodate this electronic transformation. Zheng and co-workers[1] have suggested that this conformation change (from compact coil to expanded coil[3]) is initiated by a proton-doping mechanism which generates (without loss of electrons) charge carriers along the backbone. The Coulomb repulsion[2] of these polarons forces the polymer chain to adopt a more planar conformation. The result of this conformational change is a reduction of structural defects along the polyaniline chain (e.g., twisting, buckling) which increases the π orbital overlap between the phenyl π electrons and nitrogen π electrons. This in turn increases both conjugation of the chain's backbone and the polaron's delocalization length. However, due to this conformational change and greater polarity of the ionomeric form, the solubility of PANI-ES is markedly reduced in DMSO and NMP solvents compared to PANI-EB.

As with most conducting polymer materials prepared to date, the technology has been impeded by poor polymer processability . Up until the early 1990s, fully doped polyaniline was not an exception to this general rule. However, Cao and co-workers[10] recently discovered that by functionalizing the doping acid (e.g., dodecylbenzenesulfonic acid, HDBSA) and choosing a solvent that matches the solution characteristics of the acid's functionality (e.g., xylene for the case of HDBSA), a soluble *and* conducting PANI-ES is achieved. This novel approach of functionalizing the dopant rather than the polyaniline chain has brought forth a host of new sulfonic acid-based dopants and corresponding solvents. These combinations of solvent and functionalized dopants have yielded conductive PANI-ES's having different conformations and thus different conjugation lengths in both the solution and solid states. However, complete

characterization of the solution and solid states of PANI-EB and PANI-ES (doped with different functionalized sulfonic acids) has been limited for two main reasons. First, no single "inert" solvent has been found to effectively dissolve both insulating and conductive forms of polyaniline. Solvents such as sulfuric (80%), acetic (60−88%), and formic acids simultaneously act as dopant and solvent, thus compromising the characterization of both polyaniline forms. Second, most solvents that are employed to dissolve the PANI-ES are limited by the polarity of the dopant counteranion.

Most recently, the characterization of PANI-ES has been performed from *m*-cresol solutions. This mildly acidic solvent (pK_a = 10.01) has a high boiling point of 203 °C. Furthermore, *m*-cresol dissolves both PANI-ES and PANI-EB to yield a forest-green solution in both instances. Recently, MacDiarmid, Epstein, and co-workers[3,4] demonstrated the dependence of PANI-ES molecular conformation, in the solid state, upon its extended conformation in a *m*-cresol solution from which it is cast. In particular, they note that the *m*-cresol solvent acts as a "secondary dopant"[3] which aids in the formation of an expanded coil conformation. In addition, they provide [4] substantial wide-angle X-ray scattering (WAXS) evidence that this solvent promotes a molecular conformation in the solid state which is conducive to PANI-ES crystallization.

We have found that hexafluoro-2-propanol (HFIP), a low boiling point (59 °C) and mildly acidic (pK_a = 9.3) solvent, fully dissolves *both* the PANI-EB and PANI-ES forms. As with *m*-cresol, our solution viscosity and UV−vis/near-IR experiments confirm that both PANI-ES and PANI-EB, dissolved in HFIP, likewise promote an expanded coil conformation. Unlike *m*-cresol, HFIP can almost completely be removed in one step by heating under vacuum, resulting in free standing robust films that have less than 0.5% (wt/wt) residual solvent. Under these mild solvent-stripping conditions, dopant concentration and conductivity are not compromised. In contrast to *m*-cresol, HFIP solvent does not protonate or "dope" the PANI-EB form as indicated by the brick-red solutions it yields. Specifically, the PANI/HFIP solutions were seen to go through a series of color changes from PANI-EB (brick-red) to PANI-0.12-ES (orange) to half-doped PANI-0.25-ES (lime-green) and finally to fully doped PANI-0.50-ES (blue-green).[5]

In this report we show that the PANI-EB can be partially or completely doped in this inert solvent. Furthermore, evidence of HFIP enhancing to a degree the optical properties, molecular conformation, and morphology of some PANI-ES salts is presented. We have also found that this single solvent can be used to process many polyaniline emeraldine salts with different dopant sulfonate counteranions. The resulting electrical conductivities of these salts exhibit interesting dopant dependencies. Thus the HFIP solvent makes possible a full characterization of undoped and doped polyaniline properties.

II. Experimental Section

Chemical Synthesis. PANI-EB (PANI-EB I form[6]) was chemically synthesized by the oxidation of twice vacuum distilled aniline ($C_6H_5NH_2$) (Aldrich) with ferric chloride ($FeCl_3$) (EM Sciences) according to the method of Yasuda and Shimidzu.[7] The polymer was subsequently washed twice with 1.0 M HCl and then with 1.0 M NH_4OH. This doping/undoping step promotes the breakup of physical cross-links in the polyaniline chains and improves solubility. Finally, the insulating polymer was washed with distilled water, methanol,

and diethyl ether. Each wash step was carried out until the filtrate became clear and colorless. The resulting dark, free-flowing PANI-EB powder was then dried at 70 °C[8] for 12 h to remove the remaining moisture and solvent.[9] Elemental Anal. Found (%) C, 79.56; H, 4.97; N, 15.47. Calcd (%) for ($C_{24}H_{18}N_4$) C, 79.12; H 5.18; N 15.26. IR band assignments (cm^{-1}): 3390 (N−H); 1670 (C=N, quinoid structure) 1312 (C−N, benzoid structure); 1108 (H out-of-plane bending due to para link). ^{1}H NMR (300 MHz, DMSO-d_6) : δ 7.1. ^{13}C NMR (DMSO-d_6): δ 120, 135, 140, 156. Solid state NMR (50 MHz) δ 113, 121, 135, 141, 156. This base form of polyaniline was used to prepare free-standing polyaniline salt films.

Proton Acid Doping Method. The following functionalized, monosulfonic proton doping acids (Table 1) were used as received unless otherwise indicated: (a) methanesulfonic acid, 99% (HMSA), Aldrich Chemical; (b) ethanesulfonic acid, 95% (HESA), Aldrich Chemical; (c) propanesulfonic acid (HPSA), Kodak/Arcos Chemical; (d) butanesulfonic acid (HBSA), Kodak/Arcos Chemical; (e) *p*-methylbenzenesulfonic acid, certified, (HMBSA), Fisher Scientific, vacuum oven dried at 50 °C for 24 h; (f) *p*-ethylbenzenesulfonic acid, 95% (HEBSA), Aldrich Chemical; (g) dodecylbenzenesulfonic acid (HDBSA), TCI America; and (h) (±)-camphorsulfonic acid, 98% (HCSA), Aldrich Chemical, vacuum oven dried at 50 °C for 24 h.

Fully doped PANI-ES solutions were prepared by a solution doping method. Unlike the solid mixing method of doping,[10] our doping process involved first dissolving the aliphatic or aromatic sulfonic acid in HFIP solvent (Hoechst Celanese) and subsequently adding it to the dry PANI-EB powder. For example, 3.3 mmol of solid HCSA was added to 38 mL of HFIP solvent and stirred for 10 min. This acidic solution was then added to 6.5 mmol of PANI-EB and vigorously stirred for 48 h at room temperature to yield a ≈2% (wt/wt) salt solution. The dark green/blue solution was then filtered with 0.50 μm metal Waters "push" filter. Very little, if any, insoluble PANI-HCSA fractions were observed. Full protonation was achieved in HFIP solution as seen qualitatively by the dark forest-green color and determined quantitatively by S:N elemental analysis to yield molar doping ratio (e.g., sulfonic acid dopant to polyaniline = y = 0.52). It should be noted that on standing for 14 days, no visible signs of cross-linking (e.g., gelling) were seen in any of the fully doped PANI-ES solutions except for the PANI-0.50-HDBSA solution.

Film Preparation. All filtered, doped PANI-ES films were solution cast onto a Teflon-coated glass substrate and subsequently covered with a recrystallization dish to allow slow evaporation (at room temperature) of HFIP solvent for approximately 24 h.[11] By casting onto a Teflon-tape-coated glass slide and allowing a slow solvent loss, films were observed to partially delaminate off of the Teflon substrate, yielding free standing, homogeneous, dark green/black films. All films were subsequently peeled off the Teflon substrate and dried in a dynamic vacuum oven at 75 °C for approximately 24 h. According to fluorine elemental analysis (Huffman Laboratories, Golden, CO), percent residual HFIP solvent in films was less than 0.5% (wt/wt).

UV−Vis Spectroscopy. A Hewlett Packard 8452A diode array spectrophotometer was used to collect and analyze the absorption UV−vis spectra of PANI-EB in HFIP and NMP solutions. In mixed solvent experiments, 1 mL of ca. 4 × 10^{-7} M PANI-EB/HFIP solution was placed in a quartz cuvette and an appropriate amount of NMP solvent was added dropwise with stirring to this solution.

UV−Vis/Near-IR Spectroscopy. A Perkin Elmer 7700 Series Lambda 9 model UV−vis/near-IR spectrophotometer was used to collect the data, and Grams/386 level 1 v 3.0 software was used to analyze the spectra. Concentration of PANI-EB in the respective NMP and HFIP solvents was ca. 4 × 10^{-7} M.

Solution Viscosity. All viscosity measurements of unfractionated polyaniline samples were done using a No. 75 Ubbelohde viscometer from Cannon Instrument Co. The viscometer was maintained at a constant temperature of 25 °C. Typically, a solution of polyaniline/HFIP solution (e.g., 1 g/ dL) sample was filtered with a Gelman GHP Acrodisc 0.45 μm filter and injected into the viscometer's sample port and

allowed 20 min to equilibrate with the 25 °C temperature bath. Solutions were diluted inside the viscometer by adding 2.0 mL volumes of HFIP solvent to obtain desired concentration. The viscometer was shaken vigorously for ≈ 5 min after each dilution to thoroughly mix the polyaniline/HFIP solution. The average of three solution efflux times were used in calculating the inherent and reduced viscosities. From the Huggins–Kraemer plot, the intrinsic viscosity (η) was obtained by extrapolating to zero polyaniline/HFIP solution concentration.

Gel Permeation Chromatography. Molecular weight analysis by size exclusion chromatography (SEC) technique was determined on a Waters/Millipore Co. (150-C ALC/GPC) gel permeation chromatograph with an effective molecular weight range from 2000 to 1 000 000. Operation temperatures of the GPC column and detector were maintained isothermally at 35 and 30 °C, respectively. The mobile phase was a HFIP/0.01 M sodium trifluoroacetate (used as an antagglomeration additive) solution. Elution volumes were compared against poly(methyl methacrylate) (PMMA) standards (Polymer Laboratories Ltd, UK). Polymer solutions were dissolved in HFIP to a 2 mg/mL concentration. They were subsequently filtered through a 0.50 μm Waters/Millipore Co. metal filter prior to injection.

X-ray Diffraction. Wide-angle X-ray scattering of polyaniline films were collected on a Siemens X-ray diffractometer D5000 equipped with a copper X-ray source (1.544 Å, 45 kV, 40 mA) and graphite monochromator. The divergence slit, scattered radiation slit, monochromator slit and detector slit, were 2, 2, 0.2, and 0.6 mm, respectively. Data were collected from 2° to 30° 2θ at 0.04 deg/step and 10 s/step.

Four-Point-in-line Dc Electrical Conductivity. A Hewlett Packard Model 34401A multimeter (in four-point mode) was hooked up to a four-point-in-line dc conductivity[12,13] apparatus. Four nickel/silver, parallel gold-coated, spring-loaded probes (Interconnect Devices, Inc.) epoxied in a ceramic block with a 1.0 mm spacing were lowered via a micrometer so that they made direct contact with the sample's surface. During the measurement, a constant current (1 μA) was applied to the two outer probes and the voltage across two inner probes was measured. The films were found to be ohmic over the region studied (0.1–10.0 mV). Since PANI-ES are hygroscopic, all salt films were stored under dynamic vacuum until the time of measurement. The presence of water molecules has been shown to reduce the Coulombic interactions between a radical cation (i.e., polarons) charge and the respective counteranion and thus increase the delocalization of spins on the polymer backbone which affects the electrical conductivity.[14] All resistance measurements were done in air and at room temperature and converted to conductivity by the following equation:[15]

$$\rho = \frac{1}{\sigma} = \frac{V}{I} \omega \frac{\pi}{\ln 2}$$

where ρ = resistivity ($\Omega \cdot$cm), σ conductivity (S/cm), V potential difference (mV), I applied constant current (A), and ω thickness (cm). On the basis of the film dimensions, all PANI-ES samples were regarded as infinite thin sheets.[20] The reproducibility of the results was checked by measuring the resistance four times for each film. Mean values were used in the calculation of the electrical conductivity. Thickness of PANI-ES films was determined using a Sloan Dektak II surface profilemeter. Solution cast films were ≈14 μm thick.

Electron Paramagnetic Resonance. Relative spin concentrations at room temperature were determined by electron paramagnetic resonance (EPR) measurements using a Bruker ER 200 E-SRC. An EPR tube containing ≈10 mg of rectangular-shaped film was evacuated down to 1 × 10⁻⁴ for 20 min before flame sealing. All samples were analyzed under identical conditions: e.g., center field of 3485 G (250 G sweep width), microwave power at 20 mW, microwave frequency at 9.770 GHz, modulation amplitude at 4.0 G, sweep time of 100 ms and a gain of 6.3 × 10³. Using Grams 386 software, double integration calculations of the EPR peak were used to determine the *relative* amount of unpaired spin concentration.
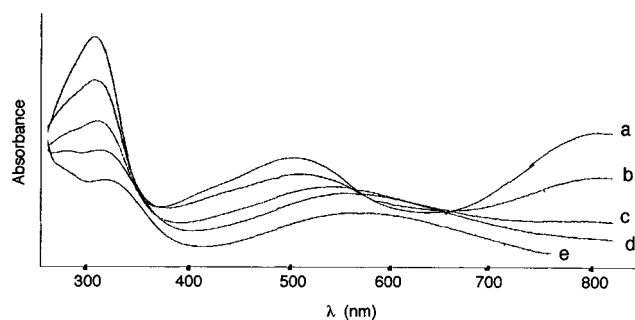

Figure 1. UV–vis absorption solution spectra of PANI-EB at 25 °C in the following mixed solvent solutions (vol/vol): (a) 100% HFIP/0% NMP; (b) 80% HFIP/20% NMP; (c) 70% HFIP/30% NMP; (d) 60% HFIP/40% NMP; and (e) 50% HFIP/50% NMP.

III. Results and Discussion

Polyaniline Emeraldine Base (PANI-EB) Form. Chain conformation plays a critical role in the properties of polyaniline.[16] We have investigated this dependency in PANI-EB using UV–vis/near-IR spectroscopy and by measuring intrinsic viscosity. Figure 1 shows the absorption spectra of PANI-EB solutions at room temperature using two solvents NMP and HFIP. Solvatochromism[17] behavior is seen when NMP is incorporated into a ≈0.2% (wt/wt) PANI-EB/HFIP solution. As shown in Figure 1a, the brick-red PANI-EB/HFIP solution has a peak at 306 nm, characteristic of the π–π^* transition,[18] an unknown peak at 502 nm, and a small "free-carrier tail" absorption at 800 nm which has been assigned to localized polaron band transitions.[9] This spectrum has some characteristic peaks of an acid-doped polyaniline but does not have the characteristic green color associated with a doped system. The tail into the near-IR region indicates that the polymer backbone adopts an expanded conformation allowing increased conjugation.

As NMP is added dropwise to this solution, both a color change (red to royal blue) and a concomitant shift and loss of absorption peaks are observed. Figure 1e is a 50–50 mixed (by volume) solvent system of NMP and HFIP. Its electronic spectrum is typical of insulating PANI-EB which has absorptions at 322 nm ascribed to the π–π^* transition electrons of the benzene ring delocalized onto nitrogen atoms of the amine and at 605 nm, assigned to excitation from the highest occupied molecular orbital (HOMO π_b) of the benzoid ring to the lowest unoccupied molecular orbital (LUMO π_q) of the localized quinoid ring.[19] No further changes are observed with additional amounts of NMP beyond the 50–50 mixture.

Such optical phenomena[20] (Figure 1) are, presumably, associated with a conformational transition of the polyaniline backbone from a more coplanar "expanded coil" structure to a more compact "coil" as a function of decreasing HFIP volume percent. The proposed mechanism by which the HFIP solvent promotes this expanded conformation of PANI-EB is the following. The mildly acidic proton in HFIP is thought to "pseudo-protonate" the imine nitrogens in PANI-EB, which creates a small population of polarons that have positive charges (that are complexed with HFIP "counteranions"). Evidence of polaron creation in the PANI-EB/HFIP solution is seen in the EPR spectrum (Figure 2a). Presumably, the HFIP solvates the complexed, slightly charged polyaniline chains, which acts to disrupt interchain interactions (i.e., decrease aggregation) and allow
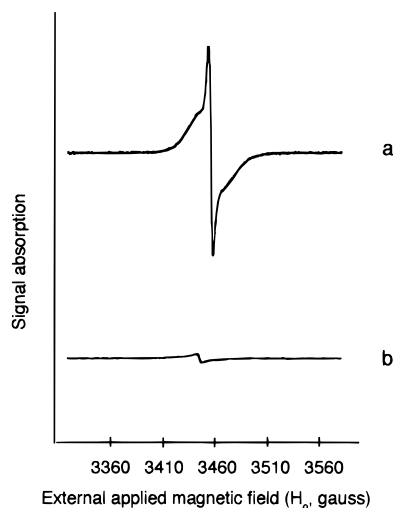
Figure 2. Electron paramagnetic resonance (EPR) of (a) 1×10^{-6} M solution of PANI-EB in HFIP and (b) PANI-EB film/powder cast from aforementioned solution.
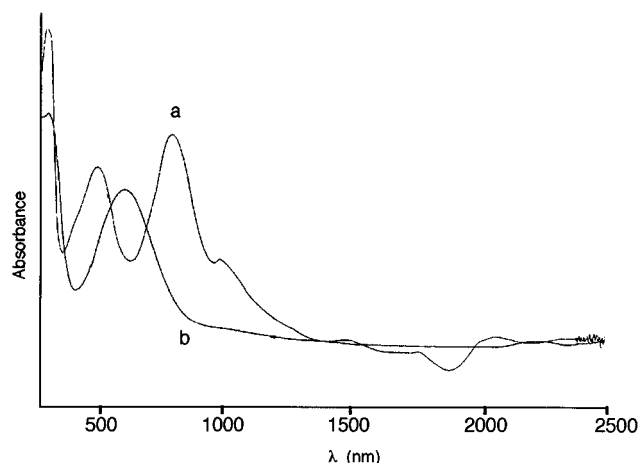

Figure 3. UV–vis/near-IR solution absorption spectra of PANI-EB in HFIP: (a) solution spectrum ($\approx$4 × 10^{-7} M) and (b) spin cast from solution and subsequently dried in a vacuum oven at 75 °C for 24 h.

the chains to adopt a more expanded conformation. In addition, the like charges on the backbone repel each other and thus further expand the PANI-EB chains to more rigid molecular conformation. Evidence of this (Figure 3a) is seen in PANI-EB's absorption into the near-IR region. Subsequent HFIP removal significantly reduces the paramagnetic behavior (Figure 2b) and the polymer is seen to revert back to its classical insulating electronic spectrum of two large absorption peaks in the UV–vis region (Figure 3b). These solid state spectra of PANI-EB confirm that the HFIP acts as an inert solvent rather than a dopant.

Figure 4 shows how the effects of *m*-cresol on PANI-EB are more characteristic of a *dopant* than simply as a *solvent*. In Figure 4a, the presence and low absorption of the free carrier tail at 2500 nm are consistent with the features of a partially doped[21] PANI-ES. Furthermore, Figure 4b shows the results of the film after attempted stripping of *m*-cresol at 100 °C for 24 h under vacuum. Most of the features associated with a doped PANI-ES salt (e.g., forest-green color of free standing film, strong absorption well into the near-IR) are still seen *after* aggressive drying/stripping conditions, suggesting that this mildly acidic molecule plays a dual role of both dopant and solvent.
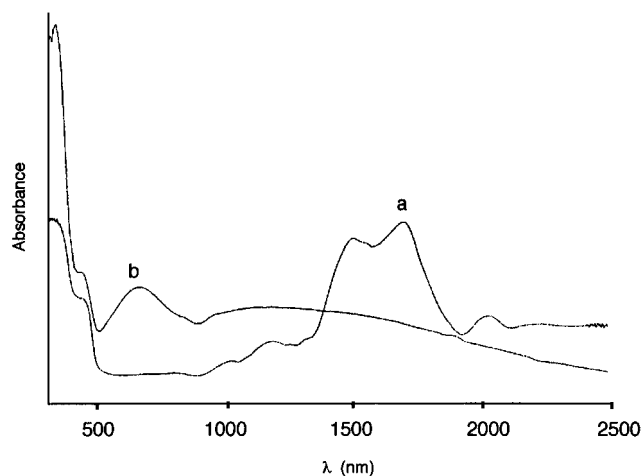

Figure 4. UV–vis/near-IR solution absorption spectra of PANI-EB in *m*-cresol: (a) solution spectrum ($\approx$4 × 10^{-7} M) and (b) spin cast from solution and subsequently dried on a hot plate at 100 °C for 24 h.

Further evidence of this expanded molecular conformation in HFIP solution was obtained from intrinsic viscosity [η] measurements. Previous solution data[2] suggests that PANI-EB chains tend to aggregate due to strong secondary interactions between polyaniline chains. Furthermore, it has been shown that in dilute regimes, PANI-ES simulates a typical polyelectrolyte behavior.[22] This behavior is noted to result from the polyaniline chain radii expanding as a result of charges on the backbone being less screened and thus repelling each other which acts to increase the viscosity of the polymer solution.[22]

When PANI-EB is dissolved in HFIP (Figure 5a), the polymer adopts an expanded conformation as seen from its larger [η] value (compared to the NMP solution, Figure 5b). It is proposed that the HFIP molecule both solvates and complexes (via pseudo-doping) polyaniline. This acts to disrupt hydrogen bonding and, as a result, the degree of aggregation between chains decreases. The combination of stronger polymer–solvent interactions (i.e., solvating power) and a pseudo-protonation of the imine nitrogens results in a Coulombic repulsion between polarons; this induces the PANI-EB chains to extend in HFIP, as evident by the increase in [η] and the absorption in the near-IR region.

Polyaniline Emeraldine Salt (PANI-ES) Form. In the above discussion we demonstrated that solvent characteristics affect the molecular conformation of the undoped polyaniline. Protonation or doping PANI-EB with either inorganic acids (e.g., HCl, H_2SO_4, etc.)[23] or organic acids (methylbenzenesulfonic acid, camphorsulfonic acid, etc.)[24] has been previously shown to further alter the backbone conformation. However, full characterization of the transition from insulating base (PANI-EB) to electrically conducting salt (PANI-ES) has been limited due primarily to solvent incompatibility of the two structurally different forms (e.g., PANI-EB and PANI-ES).

Figure 6 shows the effect of molar doping ratio (e.g., moles of doping acid:moles of phenyl-NH) or *y* on the [η] of polyaniline in HFIP. Initially, the [η] increases when PANI-EB ($y = 0$) is doped, exhibiting a maximum at $y = 0.25$ for both HESA and HEBSA dopants. This behavior is consistent with that of a polyelectrolyte in which the Coulomb repulsion interactions of the positively charged chains force the polymer backbones to adopt a more expanded molecular conformation. Inter-
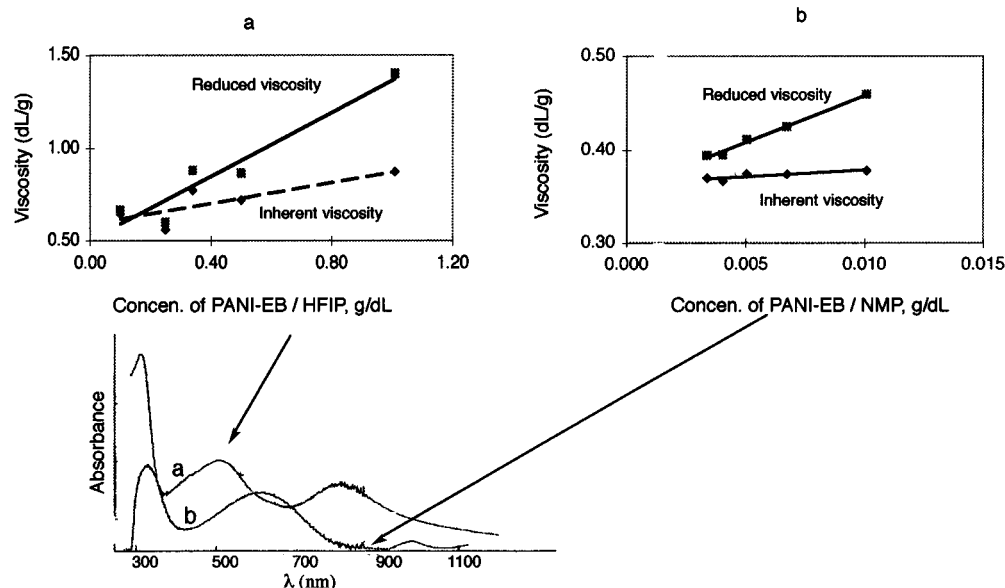
a

b

Figure 5. UV−vis/near-IR solution spectra at 25 °C of PANI-EB in (a) HFIP solvent and (b) NMP solvent. Inset figures are Huggins−Kraemer plots at 25 °C of PANI-EB in respective solvents. In (a) PANI-EB/HFIP system, $[\eta] = 0.54$ dL/g and in (b) PANI-EB/NMP, $[\eta] = 0.35$ dL/g.
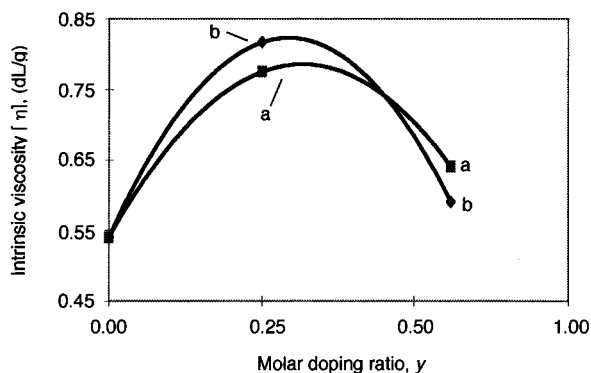

Figure 6. Intrinsic viscosity $[\eta]$ (in HFIP solvent and at room temperature) as a function of molar doping ratio, y. Dopants are (a) ethanesulfonic acid (HESA) and (b) ethylbenzenesulfonic acid (HEBSA).

estingly, along with this initial increase in solution viscosity (Figure 6), a brick-red to lime-green color change is observed when the polymer is doped to one-half the calculated optimal doping level (i.e., $y = 0.25$). As y increases to ca. 0.55, the $[\eta]$ decreases for both dopants. To a first approximation, as y increases the charge carrier density (i.e., polaron population) should increase. This should cause an increase in Coulomb repulsion, resulting in an overall expanded polyelectrolyte that increases the viscosity of the polymer solution. However, as seen in Figure 6, quite the opposite behavior happens where the $[\eta]$ is observed to saturate and then decrease as y increases. We attribute this reduction to the increase in counteranion concentration; the positive charges (polarons and bipolarons) along the polymer backbone are now shielded from one another resulting in less repulsion between polarons and thus allowing the chains to coil slightly. This behavior is in agreement with the results of Liao and co-workers[22] who noted a decrease in viscosity as they increased counteranion concentration using LiCl salt. In addition, similar behavior in $[\eta]$ for Kevlar and H_2SO_4 solutions has been observed before by Baird and Smith.[25] They attribute the saturation of $[\eta]$ to conformational changes due to excess counteranions shielding the positive charges. The η of fully doped PANI-ES ($y = 0.55$) is

observed to be slightly larger than that of the PANI-EB ($y = 0$), indicating that the fully doped polymer has adopted a larger hydrodynamic volume due to a combination of small residual charge repulsions and size contributions by the bulky dopant sulfonate counteranions. The latter effect may explain the difference in magnitude between the aliphatic and aromatic dopant's $[\eta]$ values at $y = 0.25$ and 0.55, as seen in Figure 6, a and b, respectively.

GPC measurements were used in an attempt to further confirm this coil to expanded conformational behavior using a different dopant: HCSA. In Figure 7a, the chromatogram of PANI-EB ($y = 0$) shows a fairly broad distribution of molecular weights, with a calculated M_w of 114 000 g/mol and a M_n of 26 500 g/mol. As y increases to 0.12 (Figure 7b), a very small shoulder is seen to develop at a retention time of ≈14.9 min, which corresponds to a M_w of 634 000 g/mol. As the doping increases to $y = 0.25$ (Figure 7c), the peak's intensity is seen to increase. In Figure 7d, the chromatogram of the fully doped ($y = 0.50$) PANI-HCSA salt shows no signs of this small shoulder peak and has a lower retention time with a calculated M_w and M_n of 123 300 and 37 000 g/mol, respectively. It appears that the PANI-0.50-HCSA's lower retention time (compared to PANI-EB) is due to the charged chains adopting a more elongated conformation which acts to increase the hydrodynamic volume of the polymer. However, the underlying factors that cause the development and growth of the small shoulders at ≈14.9 in Figure 6b,c are unclear. Schacklette and co-workers[26] previously observed on a molecular level that low and intermediate doping levels cause the charged polyaniline chains to separate into heavily doped and lightly doped segments or domains. In light of this, we suggest that the fully doped PANI-HCSA segments would separate from other less doped chains in the GPC column due to differences in the respective hydrodynamic volumes.

As seen in Figure 8, the solid state UV−vis/near-IR absorption spectra of PANI-y-HCSA show the changes associated with increasing the molar doping ratio from $y = 0$ to $y = 0.12$, 0.25, and 0.50. The metallic-like absorption of the "free carrier tail" at 2500 nm is seen to increase as y increases. In Figure 8d, the tail at 2500
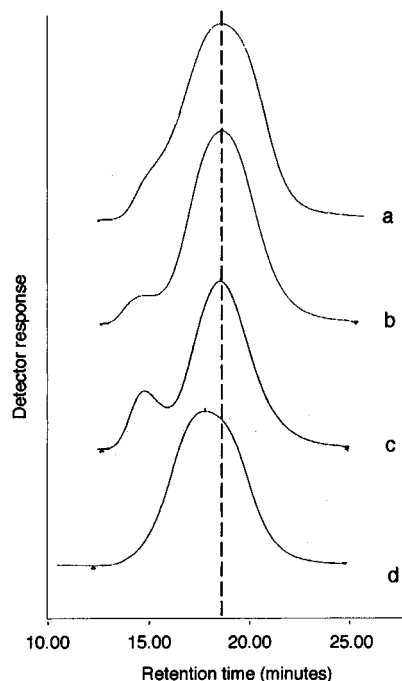
Figure 7. Gel permeation chromatography (GPC) chromatograms of PANI-y-HCSA doped at $y =$ (a) 0, (b) 0.12, (c) 0.25, and (d) = 0.50 molar doping ratios. Mobile solvent is HFIP and reference polymer is PMMA. Note: (b) is approximately 1.5 times larger than (a) and had to be reduced for comparison purposes.
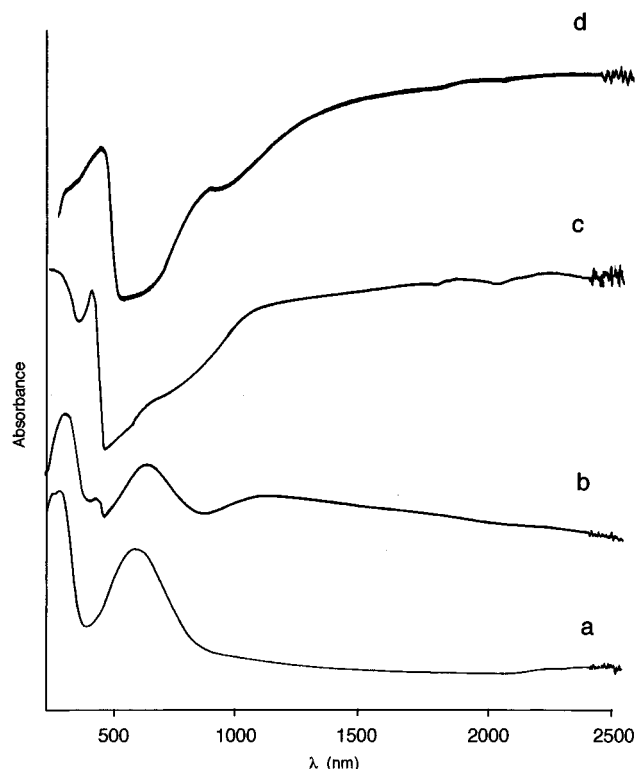

Figure 8. UV−vis/near-IR absorption spectra of PANI-y-HCSA films doped at $y =$ (a), 0, (b) 0.12 (c) 0.25, and (d) 0.50 M doping ratios. Films were spin cast from HFIP solution at 6K rpm for 2 min and subsequently vacuum oven dried at 75 °C for 24 h. Spectra have same absorption scaling.

nm along with the decrease of the 605 nm band and the appearance of the excitation peak at 440 nm[27] provide evidence of a fully protonated emeraldine salt and are also consistent with an expanded coil conformation and a longer conjugation length.

These observations are in agreement with the electronic spectra results that Xia and co-workers obtained with the PANI-0.50-HCSA/m-cresol system.[8] However, when PANI-EB is dissolved in m-cresol (Figure 4b) and spin cast/heated to remove the residual m-cresol, the resulting electronic optical spectrum of the forest-green film shows two peaks at 400 and 720 nm and a tail that stretches into the near-IR. This observation is consistent with a partially doped PANI-ES structure (Figure 8b) and suggests that m-cresol may act as both a *solvent* and a primary *dopant*. If m-cresol can act as a dopant, it may well compete with the primary acidic dopant for the imine sites on the PANI-EB chain and thus one loses precise control over stoichiometric doping of polyaniline.

By contrast, HFIP does not directly dope the PANI-EB as seen in Figure 3b. Controlled doping (Figure 8) is achieved in the HFIP which subsequently yields dark green, highly conducting, free standing films. Most importantly, less than 0.5% (wt/wt)[28] of HFIP remains after drying under relative mild conditions such as 75 °C for 24 h in a vacuum oven. More aggressive drying methods such as high heating temperatures (e.g., 200 °C) or dipping in a polar solvent (e.g., acetone or methanol) for several minutes must be utilized to "completely" eliminate m-cresol solvent from the PANI-ES. These m-cresol stripping conditions can affect the doped polyaniline and thus decrease the conductivity of the polymer at the expense of solvent removal. For instance, we observed a color change (i.e., green to blue, indicating deprotonation) when the PANI-ES films were exposed to acetone or methanol. Furthermore, since sulfonate counteranions are known to undergo desulfonation above 100 °C[29] the dopant may decompose resulting in loss of charge balance.

Wide-angle X-ray scattering (WAXS) of five unoriented polyanilines films cast from HFIP were measured at 25 °C, as seen in Figure 9. With the exception of PANI-HCSA (Figure 9e), the PANI-ES films exhibit a small amount of scattering at 18° (2θ scale), indicating a limited short-range order in the as-cast film. As seen in Figure 9a, PANI-EB film shows a broad, low intensity peak at 18° (2θ scale)) and a relatively narrow and sharp diffraction peak at a very low angle of 6° (2θ scale). This low-angle peak has been previously reported to be present only in highly crystalline (>10%) PANI-EB [30] and from using Bragg's and Scherrer's laws, interplanar distance and crystal size corresponding to this peak are ca. 13 and 274 Å, respectively. Using the mass fraction of crystals formula[31] (e.g., % crystallinity = $A_c/(A_n + A_c)$, where A_c is the scattering from sharp crystalline area peaks and A_n the scattering from noncrystalline areas, i.e., the broad underlying peak), the percent crystallinity of the undoped polymer is calculated at ≈23%.

The intensity of PANI-HCSA reflections at larger angles (e.g., 14° and 18.5° (2θ scale)) and their clear definition above the background amorphous scattering are a good indication that the CSA counteranion (in addition to the secondary interactions in the HFIP) induces a more highly crystalline film (ca. 29%), compared to the other salts surveyed. In addition to these high scattering angle peaks, the PANI-HCSA diffractograph shows a sharp diffraction peak at 4.5° (2θ scale), which corresponds to a stacking of polyelectrolyte chains that have a ca. 19 Å separation distance. The consequence of this semicrystalline morphology can be seen in its exceptionally high electrical conductivity of 385 (± 41) S/cm.
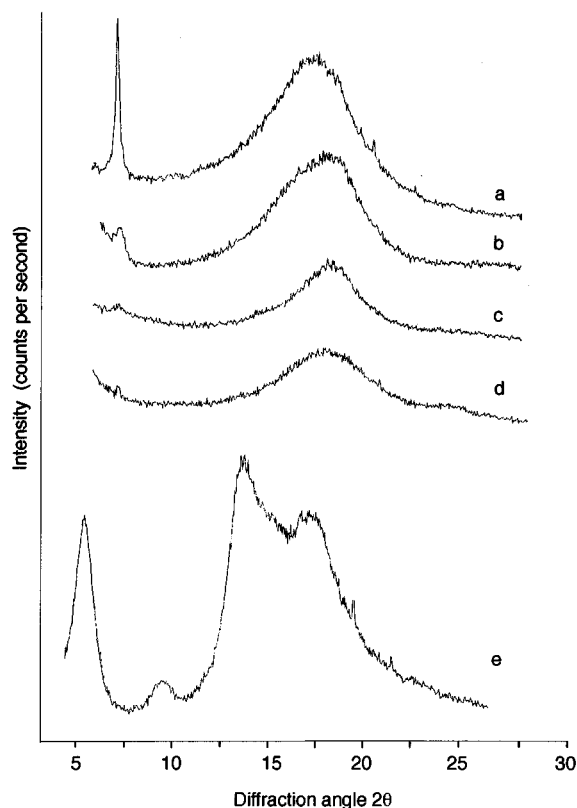
Figure 9. Wide-angle X-ray scattering (WAXS) patterns of free-standing films of (a) PANI-EB (b) PANI-HMSA, (c) PANI-HMBSA, (d) PANI-HDBSA, and (e) PANI-HCSA cast from HFIP solvent. Films were allowed to coagulate/dry for 24 h on a Teflon-coated glass substrate and subsequently vacuum oven dried at 75 °C for 24 h to remove residual HFIP solvent. Patterns are scaled to each other.

Overall, both the position and intensities of the diffraction peaks of most PANI-ES were approximately constant with the different sizes of the counteranions. For instance, the longest sulfonate counteranion (i.e., HDBSA) yielded a single, broad peak, indicating that this dopant prevents the PANI-ES chains from packing and reduces any long-range order; the shortest sulfonate counteranion (e.g., HMSA) in the study showed two small, but narrower diffraction peaks which indicates the smaller counteranion allows an increase in interchain packing and thus induces more structural order in the solid state. The aliphatic sulfonate counteranions (e.g., HMSA, HMBSA, and HDBSA) are thought to act only as "inert" spacers since they provide little or no secondary interactions with polyaniline chains. The low scattering WAXS patterns of most of the salt's surveyed indicated a low degree of interchain packing. Attempts to establish the details of why the bulky, yet hydrogen bonding, HCSA dopant consistently yields a crystalline morphology are currently underway.

Four-point-in-line dc electrical conductivities (σ_{dc}) were measured on undoped, half-doped, and fully doped polyaniline films cast from HFIP. Since this solvent has been shown to effectively dissolve both forms of polyaniline without residual protonation effects or interruption of conjugation length, it is possible to monitor the influence of the dopant's counteranion on the conductivity. For instance, since PANI-ES films carry current by a hopping mechanism, the degree of separation between charged yet spatially separated polyaniline chains may be affected by the bulkiness of the dopant's counteranion and thus could possibly disrupt stacking to crystal structure. In addition, it has been suggested
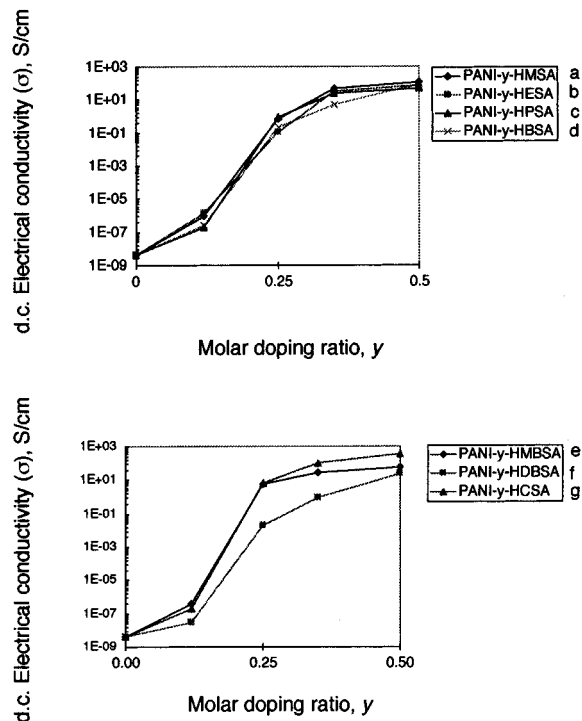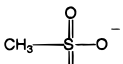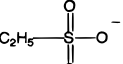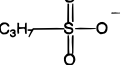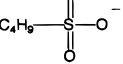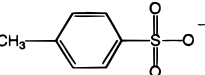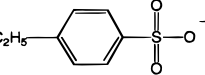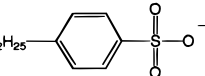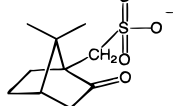

Figure 10. Four-point-in-line dc conductivity of films as a function of molar doping ratio $y = 0$, 0.12, 0.25, 0.35, and 0.50 for (a) methanesulfonic acid (HMSA), (b) ethanesulfonic acid (HESA), (c) propanesulfonic acid (HPSA), (d) butanesulfonic acid (HBSA), (e) p-methylbenzenesulfonic acid (HMBSA), (f) p-ethylbenzenesulfonic acid (HEBSA), (g) p-dodecylbenzenesulfonic acid (HDBSA), and (h) (±)-(10)-camphor sulfonic acid. Substrate for salts was a glass slide.

that the polarity of dopant counteranions is capable of disrupting conductivity by generating a significant polarization of charges in neighboring polymer chains.[32] To induce these effects, a number of aliphatic (Figure 9a–d) and aromatic (Figure 9e–h) sulfonic acids dopants with various counteranion polarities and lengths were used.

Figure 10 shows a change of approximately 9 orders of magnitude in σ_{dc} as the polymer is doped to $y = 0.25$ to yield conductivities between 0.10 and 30 S/cm (depending on sulfonate counteranion). This initial large increase in room temperature σ_{dc} marks the insulator to metal transition and onset of structural order within and between chains. The solid state electronic spectra (Figure 8, a and c) lend additional evidence to support the random coil to extended coil molecular conformation change. The charge carriers induced by this low-level doping (i.e., $y = 0.25$) readily delocalize and are thus able to carry current.

As seen in Figure 10, further doping to $y = 0.50$ increases the σ_{dc} only ≈2–3 orders of magnitude. At the fully doped level, most of the aliphatic and aromatic dopants exhibit a marginal difference in conductivities. As more clearly seen in Table 1, there are some general trends in the σ_{dc} within each family of aliphatic or aromatic functionalized dopants. The longer the alkyl group off of the functionalized sulfonic acid, the lower σ_{dc}. Furthermore, with the exception of HDBSA (Table 1h), there was no clear correlation of dopant functionality (e.g., aliphatic and aromatic) and σ_{dc}. Comparison of all the dopants surveyed showed that the sulfonate counteranion capable of hydrogen bonding (i.e., HCSA) yielded the highest σ_{dc}, (385 (±41) S/cm) while the dopant with the bulkiest alkyl group (i.e. HDBSA) yielded the lowest $\sigma_{4\ pt}$ value (25 (±4.6) S/cm).

Table 1. Dopant Counteranion in PANI-0.5-ES and Respective four-point DC Electrical Conductivity of Film Cast from HFIP Solvent

	sulfonate counter-anion:	d.c. electrical conductivity (S/cm) $\sigma_{d.c.}$ / (standard deviation)
a	CH$_3$—S—O$^-$	116 (± 3.2)
b	C$_2$H$_5$—S—O$^-$	74 (± 1.9)
c	C$_3$H$_7$—S—O$^-$	51 (± 3.5)
d	C$_4$H$_9$—S—O$^-$	85 (± 4.8)
e	CH$_3$—⬡—S—O$^-$	43 (± 2.8)
f	C$_2$H$_5$—⬡—S—O$^-$	62 (± 3.7)
g	C$_{12}$H$_{25}$—⬡—S—O$^-$	25 (± 4.6)
h	(camphorsulfonate) CH$_2$O—S—O$^-$	385 (± 41)

27

In general, doping and casting from HFIP yields PANI-ES films with σ_{dc} similar to those processed from *m*-cresol. For instance, the σ_{dc} of PANI-HCSA cast from HFIP is ca. 385 (±41) S/cm; reported PANI-HCSA values cast from *m*-cresol range from 80 to 200 S/cm, depending on residual *m*-cresol solvent content.[7]

The evolution of charge carrier density and charge mobility in the solid state as PANI-EB is gradually transformed to PANI-ES was also monitored by EPR (electron paramagnetic resonance). In Figure 10, a and b, the transition from PANI-EB to lightly doped PANI-ES is seen to increase the spin concentration and decrease the EPR peak width (ΔH_{pp}). The initial increase of paramagnetic species is primarily due to dopant-induced polaron charge carriers which marks the insulator to metal transition of the conducting polymer. In addition, the narrowing of peak width (i.e., ΔH_{pp} decrease) at low doping levels marks the onset of structural order between the charged chains that promotes a localization-to-delocalization type conversion. Further doping up to $y = 0.50$ leads to an additional increase in polaron density and delocalization. As seen in Figure 11, additional doping beyond the maximum doping level (i.e., 0.50) of polyaniline decreases both spin concentration and mobility of the polarons. This decrease in paramagnetic behavior is due to the favorable recombination[33] of polarons to form doubly charged, localized,[34] spinless bipolarons. At these high doping levels, residual polarons that did not combine to form bipolarons are seen to be localized by the observed increase in ΔH_{pp}.
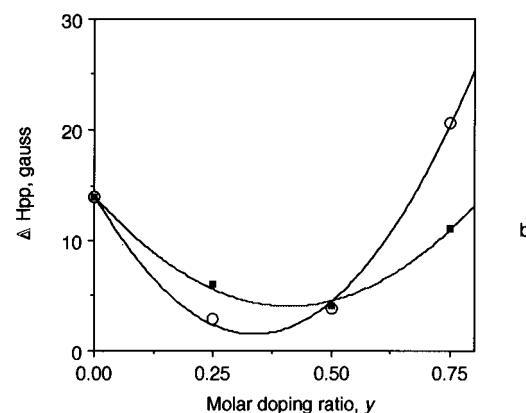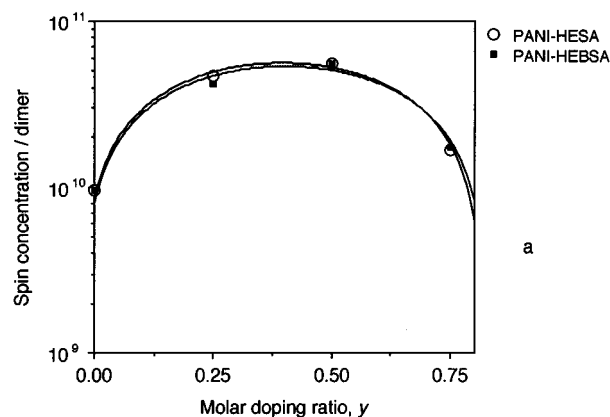
Figure 11. (a) Electron paramagnetic resonance (EPR) spin concentration and (b) ΔH_{pp} (peak to peak height) of PANI-HESA and PANI-HEBSA as a function of molar doping ratio.

IV. Conclusions

We have investigated the conformation of polyaniline as it transforms from the undoped PANI-EB to the doped PANI-ES form by the use of a non-protonating, low boiling point solvent: hexafluoro-2-propanol (HFIP). Since *both* the PANI-EB and PANI-ES readily dissolve in this inert *single* solvent, we are able to observe for the first time conformational changes as a function of the molar doping level, *y*. Absorption into the near-IR and a noticeable increase in [η] (compared to the PANI-EB/NMP solution) suggest the PANI-EB adopts an expanded coil conformation in the HFIP. It is proposed that the HFIP molecule both solvates and complexes (via pseudo-doping) the PANI-EB which reduces the degree of aggregation between polymer chains. The combination of stronger polymer–solvent secondary interactions and a pseudo-protonation of the imine nitrogens results in a Coulombic repulsion between polarons; this induces the PANI-EB chains to extend in HFIP, as evident by the increase in [η] and the absorption in the near-IR region.

When the solvent is subsequently stripped, the WAXS diffractograph shows a single sharp diffraction peak at a low angle, indicating that the induced expanded conformation of the PANI-EB chains in solution may help in stacking to crystal structure.

When PANI-EB is proton doped in HFIP solution, a slight decrease in the GPC retention time and an increase in [η] is observed. This behavior is consistent with the electrostatic repulsions of the polarons that impart a more linear PANI-ES backbone conformation which induces an increase in the solution viscosity. When HFIP is stripped from the PANI-ES salt (under

very mild conditions without compromising dopant concentration), the expanded molecular conformation is retained in the solid state, based on the strong absorption of the UV−vis/near-IR free carrier tail at 2500 nm.

This solvent effectively dissolves many PANI-ES (regardless of functionality of the sulfonate counteranion surfactant group) without residual protonation effects or interruption of conjugation length in the solid state. Thus, inherent counteranion effects on the conducting salt's morphology and conductivity can be observed. When doped from $y = 0$ to 0.25, the conductivity of most PANI-ES increases by 9 orders of magnitude, which marks the insulator to metal transition. At the fully doped level (i.e., $y = 0.50$), most of the aliphatic and aromatic functionalized dopants exhibit only a small difference in conductivities. WAXS diffractographs confirm that the morphology of most PANI-ES surveyed is amorphous. However, the PANI-HCSA diffractographs show intense reflection peaks, indicating some crystallinity in the cast film. The consequence of this semicrystalline morphology can be seen in the salt's exceptionally high electrical conductivity of 385 ($\pm$41) S/cm. We propose that a combination of solvent/polymer and increased counter-anion / neighboring polymer chain interactions (via hydrogen bonding) promotes a more extended conformation which provides the thermodynamic requirements for crystallization and the resulting high electrical conductivity.

These observations imply that there is a correlation between the functionality of the sulfonate counteranion and the final solid state properties. Furthermore, the results in this study indicate that the HFIP solvent can be used to process PANI-EB and PANI-ES with various sulfonate counteranions; in some cases, enhanced optical, conductivity, and morphology properties result from the use of this solvent.

Areas of current exploration include investigations of deuterated PANI-ES salts and blends cast from HFIP using small-angle X-ray diffraction (SAXS) and small-angle neutron scattering (SANS) techniques.

References and Notes

(1) Zheng, W.-Y.; Levon, K.; Laakso, J.; Osterholm, J. E. *Macromolecules* **1994**, *27*, 7754, 7768.

(2) Avlyanov, J. K.; Min, Y. MacDiarmid, A. G; Epstein, A. J. *Synth. Met.* **1995**, *72*, 65−71.

(3) (a) Min, Y; MacDiarmid, A. G.; Epstein, A. J. *Polym. Prepr. (Am. Chem. Soc., Div. Polym. Chem.)* **1993**, *35*, 231−232. (b)

(4) Xia, Y.; Wiesinger, J. M.; MacDiarmid, A. G.; Epstein, A. J. *Chem. Mater.* **1995**, *7*, 443−445.

(5) To see PANI-EB and PANI-ES respective solution colors, visit our web site (under Alan Hopkins) at the following address: http://www.engin.umich.edu/prog/macro.

(6) Pouget, J. P.; Jozefowicz, M. E.; Epstein, A. J; Tang, X. MacDiarmid, A. G. *Macromolecules* **1991**, *24*, 779−789.

(7) Yasuda, A.; Shimidzu, T. *Synth. Met.* **1993**, *61*, 239−245.

(8) Polyaniline, in the emeraldine base form, has been previously observed to form irreversible cross-links at ≈ 250 °C and will subsequently lose solubility. Conklin, J. A.; Juang, S.-C.; Huang, S-M.; Wen, T.; Kaner, R. B. *Macromolecules* **1995**, *28*, 6522−6527.

(9) (a) Matveeva, E. S.; Diaz Calleja, R.; Parkhutik, V. P. *Synth. Met.* **1995**, *72*, 105−110. (b) Wan, M. *J. Polym. Sci.: Part A: Polym. Chem.* **1992**, *30*, 543−549.

(10) Cao, Y.; Smith, P.; Heeger, A. J. *Synth. Met.* **1992**, *48*, 91.

(11) HFIP vapors are considered corrosive to membranes and the skin. Strong ventilation should be used along with gloves and goggles.

(12) Smits, F. M. *Bell System Tech. J.* **1957**, 711−718.

(13) Uhlir, A. **1954**, Aug, 105−128.

(14) Kahol, P. K.; Pinto, N. J.; Berndtson, E. J.; McCormick, B. J. *J. Solid State Phys. Condens. Matter* **1994**, *6*, 5631−5638.

(15) Kou-Tai, T. Ph.D. thesis, Clemson University, 1993; p 103.

(16) Ghosh, S. *Chem. Phys. Lett.* **1994**, *226*, 344−348.

(17) Wudl, F. *J. Polym. Sci.: Part B: Polym. Phys.* **1987**, *5*, 1071−1078.

(18) Lu, F. L.; Wudl, F.; Nowak, M.; Heeger, A. J. *J. Am. Chem. Soc.* **1986**, *108*, 8311−8313.

(19) Huang, W. S.; MacDiarmid A. G. *Polymer* **1993**, *34*, No. 9, 1833−1843.

(20) Roux, C.; Bergeron, J. Y.; Leclerc, M. *Polym. Prepr. (Am Chem. Soc., Div. Polym. Chem.)* **1992**, *33*, No. 2, 406−407.

(21) Wan, M. *J. Polym. Sci.: Part A: Polym. Chem.* **1992**, *30*, 543−549.

(22) (a) Gettinger, C. L.; Heeger, A. J.; Pine, D. J.; Cao, Y. *Synth. Met.* **1995**, *74*, 81−88. (b) Liao, Y. H.; Kang, T.; Levon, K. *Macromol. Chem. Phys.* **1995**, *196*, 3107−3116. (c) Jain, R.; Gregory, R. V. *Synth. Met.* **1995**, *74*, 263−266.

(23) MacDiarmid, A. G.; Chiang, J. C.; Richter, A. F.; Epstein, A. J. *Synth. Met.* **1987**, *18*, 285.

(24) Li, S.; Cao, Y.; Xue, Z. *Synth. Met.* **1987**, *20*, 141.

(25) Baird, D. G.; Smith, J. K. *J. Polym. Sci.: Polym. Chem. Ed.* **1978**, *16*, 61−70.

(26) (a) Shacklette, L. W.; Baughman, R. H. *Mol. Cryst. Liq. Cryst.* **1990**, *189*, 193. (b) Shacklette, L. W.; Wolf, J. F.; Gould, S.; Baughman, R. H. *J. Chem Phys.* **1988**, *88*, 3955.

(27) Irena, K. B. *Macromolecules* **1995**, *28*, 610−613.

(28) We find that PANI-EB, cast from NMP and subsequently heated on a hot plate for 100 °C, contains 10−12% (wt/wt) residual solvent. Using *m*-cresol to dissolve PANI-HCSA, MacDiarmid and Epstein (ref 7b within) report 12−14% tightly bound residual *m*-cresol in the salt after drying.

(29) Chan, H. S. O.; Ng, S. C.; Ho, P. K. H. *Macromolecules* **1994**, *27*, 2159−2164.

(30) Wang, F.; Tang, J.; Wang, L.; Zhang, H.; Mo, Z. *Mol. Cryst. Liq. Cryst.* **1988**, *60*, 175.

(31) Young, R. J.; Lovell, P. A. *Introd. Polym.*, **1991**, 265−266.

(32) Shacklette, L. W. *Synth. Met.* **1994**, *65*, 123−130.

(33) Bredas, J. L.; Street, G. B. *Acc. Chem. Res.* **1985**, *18*, 309−315.

(34) Scott, J. C.; Pflunger. P.; Krounbi, M. T.; Street, G. B. *Phys. Rev. B* **1983**, *28*, No. 4. 2140−2145.